# Direct Optimization of Printed Reflectarrays for Contoured Beam Satellite Antenna Applications

**Zhou, Min; Sorensen, Stig B.; Kim, Oleksiy S.; Jørgensen, Erik; Meincke, Peter; Breinbjerg, Olav**

*Published in:*
I E E E Transactions on Antennas and Propagation

*Link to article, DOI:*
10.1109/TAP.2012.2232037

*Publication date:*
2013

*Document Version*
Publisher's PDF, also known as Version of record

# Direct Optimization of Printed Reflectarrays for Contoured Beam Satellite Antenna Applications

Min Zhou, *Student Member, IEEE*, Stig B. Sørensen, Oleksiy S. Kim, Erik Jørgensen, *Member, IEEE*, Peter Meincke, *Member, IEEE*, and Olav Breinbjerg, *Member, IEEE*

***Abstract*—An accurate and efficient direct optimization technique for the design of contoured beam reflectarrays is presented. It is based on the spectral domain method of moments assuming local periodicity and minimax optimization. Contrary to the conventional phase-only optimization techniques, the geometrical parameters of the array elements are directly optimized to fulfill the contoured beam requirements, thus maintaining a direct relation between optimization goals and optimization variables, and hence resulting in more optimal designs. Both co- and cross-polar radiation patterns of the reflectarray can be optimized for multiple frequencies, polarizations, and feed illuminations. Several contoured beam reflectarrays, that radiate a high-gain beam on a European coverage, have been designed and compared to similar designs obtained using the phase-only optimization technique. The comparisons show that the designs obtained using the proposed direct optimization technique are superior in performance, both for multi-frequency and dual-polarization designs. A reflectarray breadboard has been manufactured and measured at the DTU-ESA Spherical Near-Field Antenna Test Facility to validate the proposed technique. An excellent agreement of the simulated and measured patterns is obtained.**

***Index Terms*—Accurate antenna analysis, contoured beam, optimization, pattern synthesis, reflectarray, satellite antenna.**

## I. Introduction

PRINTED reflectarrays provide a way for realizing low-cost, high-gain antennas for space applications and are the subject of increasing research interest [1]–[3]. For satellite broadcasting and telecommunication applications, where highly shaped contoured beams are required to illuminate specific geographical areas, the design requirements are extremely stringent and an accurate yet efficient design procedure is essential to meet the requirements. The shaped reflector antenna is a mature technology, both in terms of manufacturing and simulation tools, and is therefore used in many space missions to fulfill the coverage, cross-polarization, and isolation specifications. However, it suffers from large volume and mass, as well as high cost of the manufacturing, in particular the mold, which depends on the antenna requirements and can therefore not be reused for other missions. Printed reflectarrays consist of a flat surface, they are light, and for a specific coverage only the array elements are varied, thus many of the recurring costs associated with shaped reflector antennas can be eliminated. Printed reflectarrays have been used for shaped beam applications with promising results [4]–[11].

To cover the required geographical areas, the electrical size of contoured beam reflectarrays is very large, similar to shaped reflectors, and an accurate yet efficient design procedure is therefore a challenging task. Contoured beam reflectarray design is often done using a phase-only optimization technique (POT) [5], [6] which involves two steps: first, a phase-only pattern synthesis is performed to determine the phase distribution on the reflectarray surface [5], [12]; and second, the array elements are optimized, element by element, to match the phase distribution by using an analysis routine based on the spectral domain method of moments (SDMoM) [13], [14] assuming local periodicity (LP) [15], [16].

Although the POT is efficient, a direct optimization technique, where all the array elements are simultaneously optimized, can potentially produce more optimal designs. Such a technique was presented in [17]–[19] and is based on the intersection approach from [20]. In [17], a small contoured beam reflectarray was designed, fabricated, and measured. However, significant discrepancies between simulations and measurements were observed, and it was concluded that further work is needed to improve the accuracy of the reflectarray analysis. The work in [18] and [19] is an extension of the technique presented in [17] where also the position of the array elements can be included in the optimization. Since the array elements can be located in a strongly distorted grid, a full-wave method of moments (MoM) is used in the optimization. As a result, the overall synthesis becomes very time consuming.

In this work, we present a new direct optimization technique. It is efficient and has an accuracy comparable to the techniques used for the design of conventional shaped reflector antennas. It is based on a minimax optimization algorithm and the SDMoM assuming LP. To ensure an accurate, flexible, and efficient design procedure, several aspects in the analysis are taken into account. First, an accurate technique to calculate the far-field must be used [21], [22]. Second, higher order hierarchical Legendre basis functions as described in [23] are applied in the SDMoM. It is demonstrated in [24] that these basis functions yield results of the same accuracy as those obtained using singular basis functions, and they are furthermore applicable to

Manuscript received June 22, 2012; revised October 08, 2012; accepted November 25, 2012. Date of publication December 05, 2012; date of current version April 03, 2013. This work was supported by the European Space Agency (ESTEC contract No. 4000101041).

M. Zhou is with TICRA, 1201 Copenhagen, Denmark, and also with the Department of Electrical Engineering, Electromagnetic Systems, Technical University of Denmark, DK-2800 Kgs. Lyngby, Denmark (e-mail: mz@ticra.com).

S. B. Sørensen, E. Jørgensen, and P. Meincke are with TICRA, 1201 Copenhagen, Denmark (e-mail: sbs@ticra.com; ej@ticra.com; pme@ticra.com).

O. S. Kim and O. Breinbjerg are with the Department of Electrical Engineering, Electromagnetic Systems, Technical University of Denmark, DK-2800 Kgs. Lyngby, Denmark (e-mail: osk@elektro.dtu.dk; ob@elektro.dtu.dk).

Color versions of one or more of the figures in this paper are available online at http://ieeexplore.ieee.org.

Digital Object Identifier 10.1109/TAP.2012.2232037

arbitrarily shaped array elements. Finally, the incident field on each reflectarray element must be accurately represented in the SDMoM computations [25]; thus, measured near-field feed patterns are used in the calculations. The analysis accuracy has been established by comparison with measurements of reference reflectarrays.

To demonstrate the capabilities of the proposed direct optimization technique, several contoured beam reflectarrays that radiate a high-gain beam on a European coverage have been designed. They have been compared to similar designs obtained using the POT, and the comparisons show that the reflectarrays designed with the new direct optimization technique are superior in performance. A reflectarray breadboard has been manufactured at the Technical University of Denmark (DTU) and measured at the DTU-ESA Spherical Near-Field Antenna Test Facility [26]. An excellent agreement between simulations and measurements is obtained, thus validating the direct optimization technique.

The paper is organized as follows. Section II describes the direct optimization technique. The reflectarray designs are described in Section III. In Section IV, simulations are compared to the measured data, and conclusions are given in Section V.

All the computations reported in this work are carried out on a 2.8-GHz dual-core Intel processor laptop computer.

The time factor $e^{j\omega t}$ is assumed and suppressed throughout the paper.

## II. Direct Optimization Technique

The direct optimization technique (DOT) uses the same optimization procedure that is used in the TICRA software package POS [27], which is the *de facto* standard software tool for the design of shaped reflector antennas. It uses a gradient minimax algorithm for nonlinear optimization. Since it is gradient based, a good initial point is required to ensure rapid convergence and to avoid non-optimum local minima.

### A. Optimization Procedure

The contoured beam requirements are specified in a number of far-field points in the $u-v$ plane where $u=\sin\theta\cos\phi$ and $v=\sin\theta\sin\phi$. The object function $F(\boldsymbol{x})$, which consists of a set of residuals $f_i(\boldsymbol{x})$, is minimized during the optimization according to

$$\text{minimize } F(\boldsymbol{x}) = \max\{f_1(\boldsymbol{x}), f_2(\boldsymbol{x}), \ldots f_{N_s}(\boldsymbol{x})\} \quad (1)$$

where $\boldsymbol{x}$ is a vector containing the optimization variables, and $N_s$ is the number of far-field specifications. Each residual has the form

$$f_i(\boldsymbol{x}) = w_i\left(D_{\mathrm{s},i} - D_i(\boldsymbol{x})\right), \quad i=1,2,\ldots,N_{\mathrm{s}}. \quad (2)$$

Herein, $D_{\mathrm{s},i}$ and $D_i(\boldsymbol{x})$ are the specified and realized directivity, respectively, in dBi for a specified polarization component, and $w_i$ is a weight factor. The optimization variables are the geometrical parameters of the array element, e.g., side length, position, and orientation of a square patch. By optimizing the variables, the residuals are minimized and a reflectarray that best possible fulfills the coverage specifications is obtained. In this way, a direct relation between the geometrical parameters and the far-field is maintained.

The minimization of the residuals can be done simultaneously for a number of frequencies, for multiple polarizations, and for different feed illuminations, to obtain a desired bandwidth. Both co- and cross-polar radiation can be optimized, hence enabling the possibility of including cross-polar and sidelobe suppression in the optimization. The optimization of the cross-polar radiation from the entire reflectarray is an important feature as previous works on minimizing the cross-polar radiation have mostly focused on looking at the scattering response of the periodic cell [10], [28], [29] or on appropriate arrangement of the array elements [30], [31], but not by means of direct optimization of the cross-polar radiation. The optimization of the cross-polar radiation is possible in the techniques presented in [18], [19], but the results for the cross-polar radiation has not been reported.

In this paper, we restrict us to square patches located in a regular grid such that only the side lengths of the patches are used as optimization variables. Upper and lower bounds for the patches sizes are specified in the optimization. The SDMoM algorithm used in the DOT is based on [32], which is applicable for multilayer dielectric substrate configurations. In this work, only single layer configurations are considered, but the DOT can be readily applied to multilayer configurations.

### B. Far-Field Calculation

In [21], several techniques to calculate the radiation from printed reflectarrays are compared. Two techniques yielded accurate results; a Floquet harmonics technique [21, technique II], and a continuous spectrum technique [21, technique III]. Both techniques are based on the field equivalence principle [33, p. 106]. Comparison with measurements shows that an enhanced accuracy is obtained using the continuous spectrum technique, mainly in the back hemisphere. Although this technique is more accurate, it is not suited for optimization purposes, since it requires higher computation time and storage. Consequently, the Floquet harmonics technique has been selected for the calculation of the far-field during the optimization. However, for the evaluation of the final optimized reflectarray, the far-field is calculated using the continuous spectrum technique. For completeness, the Floquet harmonics technique is described in detail in the following.

Equivalent currents are calculated in the plane of the array elements and assumed to be zero on the back side and at the edges of the reflectarray. The electric and magnetic equivalent currents of array element $n$ are defined by

$$\boldsymbol{J}_{\mathrm{S}}^n = \hat{n}\times\boldsymbol{H}^n, \quad (3a)$$

$$\boldsymbol{M}_{\mathrm{S}}^n = -\hat{n}\times\boldsymbol{E}^n \quad (3b)$$

where $\boldsymbol{E}^n$, $\boldsymbol{H}^n$ are the total electric and magnetic fields on the top surface of the $n$th unit-cell, and $\hat{n}$ is the outward normal unit vector to that surface. The electric and magnetic fields $\boldsymbol{E}^n$, $\boldsymbol{H}^n$ are computed by the fundamental Floquet plane wave harmonic of the SDMoM formulation [21].

In the SDMoM computations, each array element is assumed to be illuminated by a locally plane wave. To obtain an accurate representation of the incident field, a spherical wave expansion of measured or accurately simulated feed patterns is used to compute the polarization, amplitude, and phase of the incident plane wave on each array element. The total tangential electric field on the unit-cell surface is given by

$$\boldsymbol{E}_{\mathrm{t}}^{n} = \boldsymbol{E}_{\mathrm{s,t}}^{n} + \boldsymbol{E}_{\mathrm{i,t}}^{n} = (\overline{\boldsymbol{S}}_{n} + \overline{\boldsymbol{I}})\boldsymbol{E}_{\mathrm{i,t}}^{n} \tag{4}$$

where $\boldsymbol{E}_{\mathrm{s,t}}^{n}$ is the tangential components of the scattered plane wave of array element $n$, $\boldsymbol{E}_{\mathrm{i,t}}^{n}$ is the tangential components of the incident plane wave on array element $n$, $\overline{\boldsymbol{I}}$ is the identity matrix, and $\overline{\boldsymbol{S}}_{n}$ the scattering coefficient matrix which is calculated using the fundamental Floquet harmonic. The magnetic field $\boldsymbol{H}^{n}$ can be readily obtained using the plane wave relation.

The reflectarray far-field can be computed as a sum of the contributions of each array element

$$\boldsymbol{E}_{\mathrm{far}} = \sum_{n=1}^{N\mathrm{e}} \boldsymbol{E}_{\mathrm{far}}^{n} \tag{5}$$

where $N_{\mathrm{e}}$ is the number of array elements. Since $\boldsymbol{E}^{n}$, $\boldsymbol{H}^{n}$ are plane waves, the integral involved in calculating the far-field contribution from array element $n$ can be evaluated analytically for rectangular cells as

$$\boldsymbol{E}_{\mathrm{far}}^{n}(\hat{r}) = \frac{jk_0^2 u_x u_y}{4\pi}\left[\left(\left(\boldsymbol{J}_0^{n}\cdot\hat{r}\right)\hat{r} - \boldsymbol{J}_0^{n}\right)\eta_0 + \hat{r}\times\boldsymbol{M}_0^{n}\right] \cdot\mathrm{sinc}\left(\frac{\left(k_0 u - \beta_x^{n}\right)u_x}{2}\right)\mathrm{sinc}\left(\frac{\left(k_0 v - \beta_y^{n}\right)u_y}{2}\right)e^{jk_0\hat{r}\cdot\boldsymbol{r}_n}. \tag{6}$$

Herein, $k_0$ is the free-space wavenumber, $\eta_0$ the free-space impedance, $\hat{r}$ the unit vector towards the observation point, $u_x$, $u_y$ the $x$ and $y$ dimensions of the unit-cell, $\beta_x^{n}$, $\beta_y^{n}$ the $x$ and $y$ components of the propagation vector of the fundamental Floquet harmonic for array element $n$, $\boldsymbol{r}_n$ the position of array element $n$, $\boldsymbol{J}_0^{n}$ and $\boldsymbol{M}_0^{n}$ the complex amplitudes of $\boldsymbol{J}_{\mathrm{S}}^{n}$ and $\boldsymbol{M}_{\mathrm{S}}^{n}$, respectively, and $\mathrm{sinc}(x) = \sin x/x$.

This procedure corresponds to constructing equivalent currents on the surface, $S$, which is covered by all the elements/unit-cells. It was shown in [21], [22] that the finite extent of the reflectarray has to be taken into account to ensure an accurate radiation pattern in the forward hemisphere. For practical reasons, the substrate and ground plane in reflectarrays are often extended at the edges, and the physical substrate size is usually larger than $S$. To correct for this, unit-cells with no array elements are placed at the edges such that the extended substrate area $S_{\mathrm{ext}}$ is also covered. The electric and magnetic fields scattered by these empty unit-cells, which are readily obtained from the reflection of the incident field, are then used to form the equivalent currents on $S_{\mathrm{ext}}$. In this way, equivalent currents are constructed on the entire surface $S_{\mathrm{tot}} = S + S_{\mathrm{ext}}$, yielding accurate radiation patterns in the forward hemisphere. More details can be found in [21], [22].

### C. Choice of Basis Functions

To ensure an accurate yet efficient calculation of $\overline{\boldsymbol{S}}_{n}$, suitable basis functions must be selected to reduce the number of basis functions and Floquet harmonics. For canonically shaped array elements e.g., rectangular patches, entire domain singular basis functions with the correct edge conditions are known to provide fast convergence in the SDMoM with respect to the number of basis functions [34]–[36]. However, due to their singular behavior, the Fourier spectrum is wide, which increases the number of Floquet harmonics. For arbitrarily shaped elements, the common choices are first-order basis functions, e.g., Rao–Wilton–Glisson (RWG) [37] or rooftop [38] basis functions. However, the number of basis functions is high for these cases.

In this work, higher-order hierarchical Legendre basis functions as described in [23] are applied in the SDMoM. It was demonstrated in [24] that these basis functions are capable of giving results of the same accuracy as those obtained using entire domain singular basis functions. Furthermore, higher-order hierarchical Legendre basis functions can be applied to arbitrarily shaped array elements with improved performance compared to first-order basis functions. The flexibility of the higher-order hierarchical Legendre basis functions enables the optimization of reflectarrays consisting of non-canonical element shapes, e.g., those reported in [39]–[41], which is important in the analysis of printed reflectarrays.

### D. Scattering Matrix Lookup Table

Although the SDMoM combined with LP and higher order hierarchical Legendre basis functions is computationally efficient with only a fraction of a second in computation time per array element, it is not fast enough for optimization where the analysis must be performed repeatedly. Furthermore, the optimization requires derivatives with respect to the optimization variables, which will further increase the computation time if these derivatives have to be computed numerically by finite difference approximations.

To circumvent the calculation of scattering matrices of all array elements at each iteration, the scattering matrices can be calculated in advance and stored in a lookup table which is accessed during the optimization. This approach has been successfully used in other works [10], [18], [19], [42] and is also used here in the DOT. The scattering matrix is a function of many parameters, e.g., illumination angles $(\theta^{\mathrm{i}}, \phi^{\mathrm{i}})$, geometry of the array element, unit-cell dimensions, dielectric substrate properties, and frequency. It is thus important to find an economic way to store and interpolate these data to obtain a lookup table that is small and fast to compute.

The representation of the scattering matrices can be done in various ways, e.g., splines. However, due to the resonance properties of printed elements, the scattering matrix has a strong variation at resonance, hence splines are unsuited. The representation of the scattering matrices by means of local cubic interpolation [43, Chap. 25] on the other hand is efficient and stable. We have found that a sufficient accuracy can be obtained using relatively few scattering matrix sample values. For a center fed $20\lambda_0 \times 20\lambda_0$, with $\lambda_0$ being the free-space wavelength, reflectarray consisting of square patches and a focal distance to diameter ratio $(F/D)$ of one, approximately $N_{\mathrm{el}} = 60$ patch sizes and $N_\theta = 12$ sample values in $\theta^{\mathrm{i}}$ are adequate. The variation

of the scattering coefficients in $\phi^{\mathrm{i}}$ can be represented by a finite Fourier series expansion

$$\overline{\boldsymbol{S}}(\theta^{\mathrm{i}},\phi^{\mathrm{i}}) = \sum_{s=-N_{\mathrm{m}}}^{N_{\mathrm{m}}} \overline{\boldsymbol{c}}_s(\theta^{\mathrm{i}}) e^{js\phi^{\mathrm{i}}}. \tag{7}$$

The Fourier coefficients $\overline{\boldsymbol{c}}_s$ can be computed exactly by [44, App. A4]

$$\overline{\boldsymbol{c}}_s = \frac{\Delta\phi}{2\pi} \sum_{l=1}^{2N_{\mathrm{m}}+1} \overline{\boldsymbol{S}}\left(\theta^{\mathrm{i}},\phi_l^{\mathrm{i}}\right) e^{-js\phi_l^{\mathrm{i}}} \tag{8}$$

where $\Delta\phi = 2\pi/(2N_{\mathrm{m}}+1)$ and $\phi_l^{\mathrm{i}} = \Delta\phi(l-1)$. We have found that $N_{\mathrm{m}} = 2$ is sufficient, resulting in a total of only $N_\phi = 5$ sample values in $\phi^{\mathrm{i}}$. Thus for a given frequency, substrate, and unit-cell size, the total number of scattering matrix samples needed in the look-up table to obtain an accurate interpolation is $N_{\mathrm{total}} = N_\theta N_\phi N_{\mathrm{el}} = 12 \cdot 5 \cdot 60 = 3600$. Each scattering matrix sample contains four 16 byte complex numbers, thus resulting in a lookup table of a total size of only 225 kB per frequency. The computation time to calculate the lookup table for one frequency is approximately two minutes. For reflectarrays with other dimensions or feed positions, $N_\theta$ and $N_\phi$ may differ, but $N_{\mathrm{el}}$ remains the same.

For array elements with several adjustable parameters, the total number of scattering matrices samples per frequency increases rapidly as it becomes $N_{\mathrm{total}} = N_\theta N_\phi N_{\mathrm{el}}^1 N_{\mathrm{el}}^2 \ldots N_{\mathrm{el}}^{N_l}$, where $N_l$ is the number of adjustable parameters. This increases the computation time and the storage requirements of the lookup table significantly. For example, an array element with three adjustable parameters which are optimized for three frequencies gives $N_{\mathrm{total}} = 13 \cdot 10^6$, yielding a storage requirement of approximately 2 GB. However, once the lookup table has been calculated, it can be reused in the optimization and needs only to be recalculated if another substrate, frequency, or unit-cell size is used.

Using local cubic interpolation, the derivatives with respect to the geometrical parameters of the array element can be computed by differentiation of the local cubic polynomial. Thus, the gradients needed during the optimization can be determined analytically, which is more accurate and faster than numerical difference approximations.

### *E. Phase-Only Optimization Technique*

In order to avoid the optimization being trapped in a local minimum, a good starting point is required. Depending on the complexity and the requirements of the specified contour, identical array elements can be used as the starting point. This produces an initial pattern that resembles the feed pattern and is a good initial start in certain cases, e.g., multi-frequency designs. Another choice is to use an initial defocused elliptical beam obtained by a proper phase variation over the reflectarray surface. However, this is problematic for multi-frequency designs as the phases depend on the frequency. On the other hand, for single frequency designs an elliptical beam can be a very good starting point.

Alternatively, a reflectarray designed using the POT can be used as the starting point. The POT is simple and fast and is the commonly used method for the design of contoured beam reflectarrays [5], [6], [10], [11]. First, a phase-only pattern synthesis is performed to determine the phase distribution required on the reflectarray surface, and hereafter the array elements are determined, element by element, to match the phase distribution. Although the technique is simple and has proven to be useful, it suffers from the disadvantage that intermediate optimization steps are necessary to fulfill a given phase distribution. This intermediate step breaks the direct relation between the geometrical parameters and the far-field performance and can give non-optimal designs. A brief outline of our POT implementation is given in the following.

To obtain the phase distribution on the reflectarray surface, an approach similar to that described in [12] is used. For dual-polarized multi-frequency designs, several phase distributions are obtained, one for each polarization and frequency. The array elements are subsequently optimized, element by element, to comply with these phase distributions by minimizing the error function

$$e_n = \sum_{l=1}^{L} C_l \left|\psi_{n,r}^l - \psi_{n,c}^l\right|. \tag{9}$$

Herein, $L$ is the number of phase distributions, $\psi_{n,r}^l$ and $\psi_{n,c}^l$ the required and computed phase-shift, respectively, of array element $n$, and $C_l$ weighting coefficients, which can be different for each phase distribution. The selection of $C_l$ is usually done empirically to obtain the best performance of the optimized design.

To find array elements that match all phase distributions simultaneously is in most cases not possible. Consequently, the array elements are determined as a compromise between the different phase distributions, resulting in non-optimal designs.

## III. Reflectarray Design

To demonstrate the capabilities of the DOT and its advantages against POT, we consider several offset contoured beam reflectarrays that radiate a high-gain beam on a European coverage with the possibility of having sidelobe suppression within a southern African contour. The coverages are shown in Fig. 1 as red polygons. The reflectarray parameters are summarized in Table I with respect to the coordinate system shown in Fig. 2.

Square patches are used in these designs. Although these array elements may not provide the most optimal designs, they are sufficient for the comparison of the different design techniques.

Two reflectarray designs are considered; a multi-frequency single-polarized reflectarray design, and a single frequency dual-polarized reflectarrray design. The design process for the two cases are described in the following sections.

### *A. Multi-Frequency Single-Polarized Reflectarray*

The goal of this design is to maximize the directivity within the European coverage in the frequency range 9–11 GHz for a single feed polarization. A linearly polarized Gaussian beam with a taper of $-15$ dB at 30° is used as feed.

Two reflectarrays were designed, one using the POT, and one using the DOT. A scattering matrix look-up table for frequen-

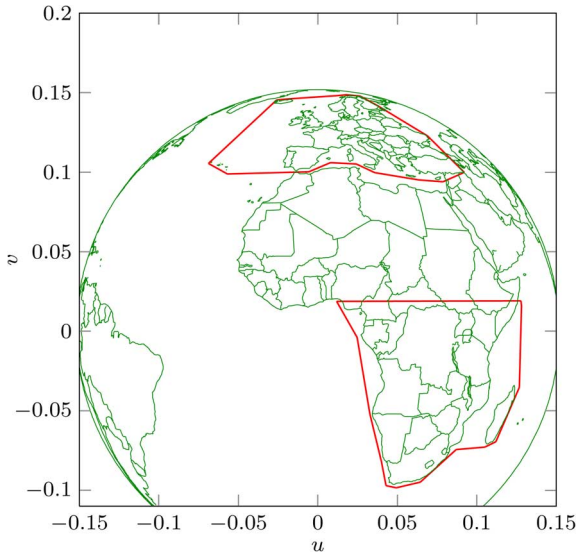


Fig. 1. European and southern African coverages seen from the longitude 0° geostationary orbital position.

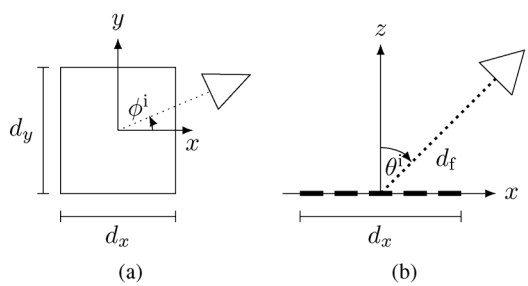


Fig. 2. Reflectarray geometrical parameters in (a) the $xy$-plane and (b) the $xz$-plane.

TABLE I
REFLECTARRAY DATA

| | |
|---|---|
| Center frequency | 10 GHz |
| Frequency range | $9-11$ GHz |
| Number of elements | 50×50 |
| Reflectarray dimensions | 600 mm × 600 mm |
| Relative permittivity | $\epsilon_{\mathrm{r}}=3.66$ |
| Substrate thickness | $d=1.524$ mm |
| Loss tangent | $\tan\delta=0.0037$ |
| Feed distance to center of array | $d_{\mathrm{f}}=0.6$ m |
| Feed offset angle | $\theta^{\mathrm{i}}=30°$, $\phi^{\mathrm{i}}=0°$ |

cies $f$ =9, 10, 11 GHz has been calculated using a total computation time of approximately five minutes and a storage requirement of 1.1 MB.

For the POT design (Design A-I), phase distributions at the center and the extreme frequencies were obtained and subsequently used in the minimization of (9) with $l$ =1, 2, 3 corresponding to $f_l$ =9, 10, 11 GHz, respectively. The optimization process was repeated several times, alternating $C_l$ to obtain the optimal performance within the frequency range. The best design showed a minimum directivity within the coverage of 25.4 dBi in the entire frequency range.

For the DOT design (Design A-II), identical patches was used as the starting point for the optimization. The reflectarray was optimized at the center and extreme frequencies simultaneously. The radiation pattern of Design A-II at 10 GHz is shown in Fig. 3 where a minimum directivity of 26.8 dBi is achieved.

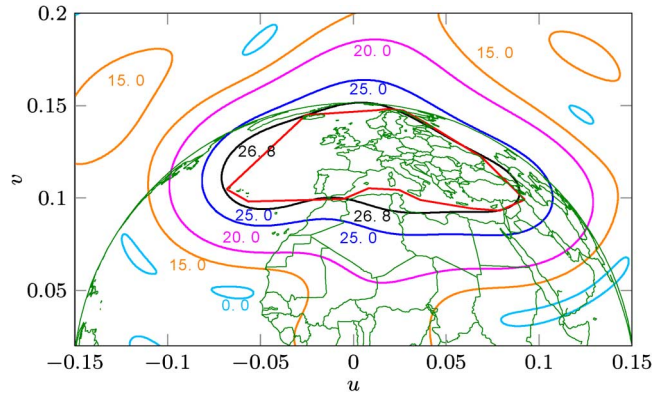


Fig. 3. Simulated co-polar radiation patterns of Design A-II at 10 GHz.

TABLE II
PERFORMANCE OF MULTI-FREQUENCY REFLECTARRAY DESIGNS

| Frequency (GHz) | Design A-I POT: Minimum Directivity (dBi) | Design A-II DOT: Minimum Directivity (dBi) |
|---|---|---|
| 8.5 | 24.2 | 24.9 |
| 9.0 | 25.4 | 26.5 |
| 9.5 | 25.5 | 26.7 |
| 10.0 | 25.4 | 26.8 |
| 10.5 | 25.4 | 26.6 |
| 11.0 | 25.4 | 26.5 |
| 11.5 | 23.2 | 23.4 |

In Table II, the performance of the two designs are summarized. A comparison clearly shows the advantages of the DOT, where more than 1 dB in the minimum directivity is gained compared to the phase-only design. Also, the phase-only design is highly dependent on the value of $C_l$, which have to be obtained empirically. This is circumvented in the DOT.

For Design A-I, the computation time was approximately 20 minutes for a fixed set of $C_l$. The optimization time for Design A-II was approximately 30 minutes.

It should be noted that the phase of the scattered field for a periodic array of square patches is known to be very sensitive to frequency variations near the resonance, thus resulting in a narrow bandwidth [16], [41]. Nonetheless, Design A-II has been optimized to have a minimum directivity of 26.5 dBi in a frequency bandwidth of 20%. It is expected that better results can be achieved by using more broadband array elements, e.g., the ones proposed in [39] or multilayer configurations as in [5], [16].

### *B. Single-Frequency Dual-Polarized Reflectarray*

In this example, we consider a high-gain beam on the European coverage with cross-polar suppression within the same coverage, and sidelobe suppression within the southern African contour. The reflectarray is optimized for two orthogonal linear polarizations, H- and V-polarization,[1] and only at 10 GHz. For this design, a corrugated horn, whose measured radiation pattern is available, is used as a feed. Again, two reflectarrays were designed, one using the POT, and one using the DOT.

[1]The reflectarray is assumed to be mounted on a satellite such that H-polarization is defined to be in the feed offset plane [$xz$-plane in Fig. 2(b)], and V-polarization in the orthogonal plane.

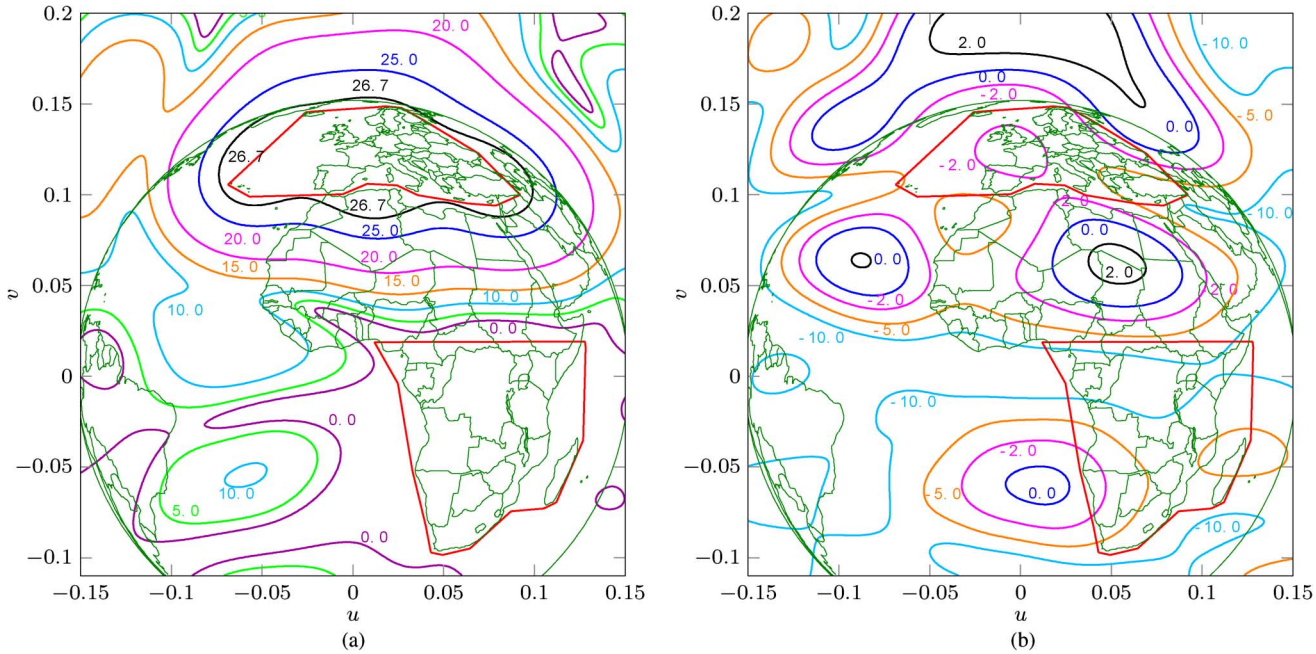


Fig. 4. Simulated (a) co-polar and (b) cross-polar radiation pattern of Design B-II for H-polarization at 10 GHz.

TABLE III
PERFORMANCE OF DUAL-POLARIZED REFLECTARRAY DESIGNS AT 10 GHz

| | Design B-I | | Design B-II | |
|---|---|---|---|---|
| | POT: | | DOT | |
| | H-pol. | V-pol. | H-pol. | V-pol. |
| Min. directivity (dBi) | 26.6 | 26.5 | 26.7 | 26.5 |
| Min. XPD (dB) | 26.5 | 26.7 | 28.6 | 27.0 |
| Min. isolation (dB) | 20.3 | 24.3 | 26.7 | 27.9 |

For the POT design (Design B-I), two phase distributions were determined, one for each polarization. In [11], rectangular patches were used and the optimization for the two orthogonal polarizations was accomplished by adjusting the two orthogonal dimensions of the rectangular patches. In our design, square patches are used and only one dimension can be varied. Thus, the optimization for the two polarizations is done simultaneously by minimizing (9) with $l = 1, 2$ corresponding to H- and V-polarization, respectively. The $C_l$ were selected to be identical in this case.

The far-field showed a minimum directivity within the coverage of 26.5 dBi and a minimum cross polarization discrimination (XPD) around 26.5 dB for both polarizations. For the co-polar radiation on the southern African coverage, the minimum isolation (Europe/Africa) for H- and V-polarization is 20.3 dB and 24.3 dB, respectively.

For the DOT design, an elliptical beam was used as the starting point for the optimization. The radiation pattern of this optimized design (Design B-II) for H-polarization at 10 GHz is shown in Fig. 4. It is seen that a minimum directivity of 26.7 dBi is obtained. The minimum XPD and isolation levels are at 28.6 dB and 26.8 dB, respectively. For the V-polarization, the design has a very similar performance.

The performance of the designs is compared in Table III. The comparison shows that a better design is achieved using the DOT than with the POT. However, the improvements are not as significant as for the case of the multi-frequency design. This is explained by the fact that the phase distributions required for the two polarizations used in the POT are rather similar. Thus the minimization of the error function does not possesses the same complexity as it does for a multi-frequency design.

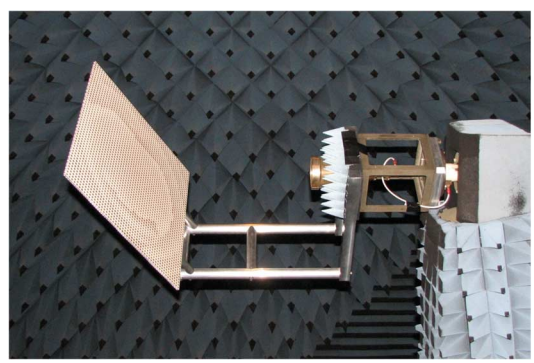

Fig. 5. Reflectarray breadboard in the DTU-ESA spherical near-field antenna test facility.

The overall optimization time for Design B-I was around 15 minutes, whereas the overall optimization time, including the calculation of the lookup table, for Design B-II was approximately 40 minutes.

It is a known fact that the response of a periodic array of square patches is different under oblique incidence [45]. As a result, the response for each orthogonal polarization is slightly different and the dimensions of the square patches are determined as a compromise between the two polarizations. It is expected that an enhanced performance can be achieved using rectangular patches.

## IV. VALIDATION BY MEASUREMENTS

To validate the DOT, a reflectarray breadboard has been manufactured at the Technical University of Denmark (DTU) and measured at the DTU-ESA Spherical Near-Field Antenna Test Facility [26], see Fig. 5. The breadboard is based on an earlier

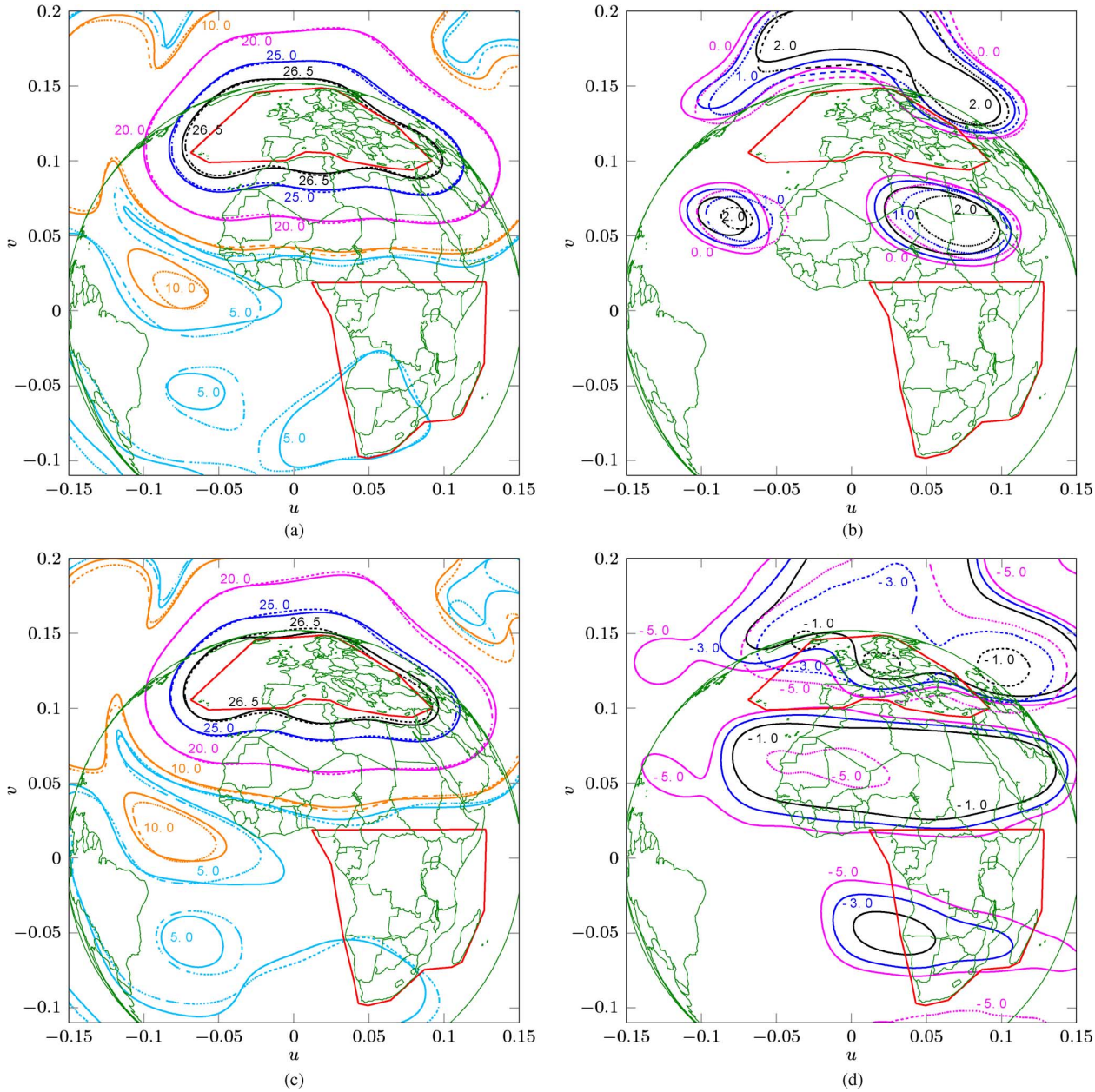


Fig. 6. Simulated (solid lines) and measured (dotted lines) radiation patterns of the manufactured breadboard for both H- and V-polarizations at 10 GHz. (a) H-polarization, co-polar; (b) H-polarization, cross-polar; (c) V-polarization, co-polar; (d) V-polarization, cross-polar.

version of Design B-II, where the performance of the reflectarray is not optimal. Nevertheless, it is sufficient to serve as reference to verify the accuracy of the proposed technique. The dielectric substrate is Rogers RO4350B with a substrate thickness of $d = 0.762$ mm. The breadboard was measured at a series of frequencies from 9.6 GHz to 10.5 GHz. For the peak directivity, the measurements have a $1\sigma$ uncertainty of 0.05 dB.

To account for the presence of the support structures, the scattering from the struts is included in the simulations using the MoM add-on in GRASP [46].

The simulated and measured radiation patterns at 10 GHz for V- and H-polarization are shown in Fig. 6. The agreement between simulations and measurements is extremely good for both polarizations. It is seen that the high-gain contours curves practically coincide.

TABLE IV
MEASURED VERSUS SIMULATED DATA AT 10 GHz

| | Peak directivity (dBi) | Min. directivity (dBi) | Min. XPD (dB) | Min. isolation (dB) |
|---|---|---|---|---|
| Measurement (H-pol.) | 28.3 | 26.5 | 27.1 | 17.5 |
| Simulation (H-pol.) | 28.2 | 26.6 | 25.0 | 17.8 |
| Measurement (V-pol.) | 27.9 | 26.5 | 27.7 | 18.4 |
| Simulation (V-pol.) | 27.9 | 26.5 | 25.5 | 17.2 |

The performance of the breadboard for both polarizations is summarized in Table IV. It is seen that an excellent agreement is obtained for the peak directivity and minimum directivity within the European coverage. Also the isolation levels are in good agreement.

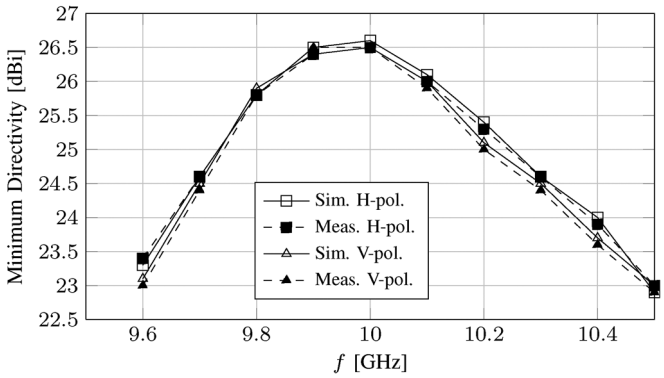


Fig. 7. Measured versus simulated minimum directivity for both polarizations for the measured frequencies.

Regarding the XPD levels, discrepancies up to approximately 2 dB are observed. This is expected since the cross-polar level is approximately 30 dB below the co-polar peak, and factors e.g., scattering from the edges come into play.

In Fig. 7, the simulated and measured minimum directivity for both polarizations are shown for the measured frequencies. The breadboard was only optimized at 10 GHz, hence the decrease in the minimum directivity in the frequency range. The maximum deviation between simulations and measurements is within $\pm 0.1$ dB, thus demonstrating the good agreement between simulated and measured patterns in the other measured frequencies.

These excellent agreements between simulated and measured patterns are close to those obtained for conventional shaped reflectors and thereby verify the direct optimization technique presented in this paper.

## V. Conclusion

An accurate and efficient direct optimization technique for the design of contoured beam reflectarrays is presented. It is based on the spectral domain method of moments (SDMoM) with local periodicity and a minimax optimization algorithm. Contrary to the conventional phase-only optimization techniques, the geometrical parameters of the array elements are directly optimized to fulfill the contoured beam requirements, thus maintaining a direct relation between optimization goals and optimization variables. As a result, more optimal designs can be obtained. To ensure high accuracy, efficiency, and flexibility, higher order hierarchical Legendre basis functions are used together with a fast yet accurate far-field calculation technique. The higher order hierarchical Legendre basis functions can give results of the same accuracy as those obtained using entire domain singular basis functions, and are applicable to any arbitrarily shaped array elements. The far-field calculation technique uses scattering matrices which are calculated in advance, stored in a lookup table, and accessed during the optimization. This circumvents the calculation of the SDMoM at each iteration and greatly reduces the overall optimization time. Both co- and cross-polar radiation can be optimized for multiple frequencies, polarizations, and feed illuminations.

To demonstrate the capabilities of the direct optimization technique, several contoured beam reflectarrays that radiate a high-gain beam on a European coverage have been designed, and compared to similar designs obtained using a phase-only optimization technique. The comparison shows that the direct optimized designs are superior in performance, both for multi-frequency and dual-polarization designs. Particularly for multi-frequency designs where more than 1 dB in the minimum co-polar directivity within the coverage can be gained. To validate the results, a reflectarray breadboard has been manufactured and measured at the DTU-ESA Spherical Near-Field Antenna Test Facility. An excellent agreement is obtained for the simulated and measured patterns, where the maximum deviation in the minimum directivity between simulations and measurements is within $\pm 0.1$ dB.

## Acknowledgment

The authors would like to thank Dr. S. Pivnenko, Electromagnetic Systems, Technical University of Denmark (EMS-DTU), for the accurate measurements of the reflectarray breadboard, the mechanical workshop at EMS-DTU for the manufacturing of the reflectarray breadboard, and Dr. G. Toso, ESA-ESTEC, for providing valuable technical comments.

## References

[1] J. Huang and J. A. Encinar, *Reflectarray Antennas*. New York, NY, USA: IEEE Press, 2008.

[2] J. A. Encinar, "Recent advances in reflectarray antennas," in *Proc. EuCAP*, Barcelona, Spain, 2010.

[3] A. Roederer, "Reflectarray antennas," in *Proc. EuCAP*, Berlin, Germany, 2009.

[4] D. M. Pozar, S. D. Targonski, and R. Pokuls, "A shaped-beam microstrip patch reflectarray," *IEEE Trans. Antennas Propag.*, vol. 47, no. 7, pp. 1167–1173, Jul. 1999.

[5] J. A. Encinar and J. A. Zornoza, "Three-layer printed reflectarrays for contoured beam space applications," *IEEE Trans. Antennas Propag.*, vol. 52, no. 5, pp. 1138–1148, May 2004.

[6] J. A. Encinar, L. S. Datashvili, J. A. Zornoza, M. Arrebola, M. Sierra-Castaner, J. L. Besada-Sanmartin, H. Baier, and H. Legay, "Dual-polarization dual-coverage reflectarray for space applications," *IEEE Trans. Antennas Propag.*, vol. 54, no. 10, pp. 2827–2837, Oct. 2006.

[7] J. Zornoza, R. Leberer, J. Encinar, and W. Menzel, "Folded multilayer microstrip reflectarray with shaped pattern," *IEEE Trans. Antennas Propag.*, vol. 54, no. 2, pp. 510–518, Feb. 2006.

[8] M. Arrebola, J. A. Encinar, and M. Barba, "Multifed printed reflectarray with three simultaneous shaped beams for LMDS central station antenna," *IEEE Trans. Antennas Propag.*, vol. 56, no. 6, pp. 1518–1527, Jun. 2008.

[9] E. Carrasco, M. Arrebola, J. A. Encinar, and M. Barba, "Demonstration of a shaped beam reflectarray using aperture-coupled delay lines for LMDS central station antenna," *IEEE Trans. Antennas Propag.*, vol. 56, no. 10, pp. 3103–3111, Oct. 2008.

[10] H. Legay, D. Bresciani, E. Labiole, R. Chiniard, E. Girard, G. Caille, L. Marnat, D. Calas, R. Gillard, and G. Toso, "A 1.3 m earth deck reflectarray for a Ku band contoured beam antenna," in *Proc. 33rd ESA Antenna Workshop*, Noordwijk, The Netherlands, 2011.

[11] J. A. Encinar, M. Arrebola, L. D. L. Fuente, and G. Toso, "A transmit-receive reflectarray antenna for direct broadcast satellite applications," *IEEE Trans. Antennas Propag.*, vol. 59, no. 9, pp. 3255–3264, Sep. 2011.

[12] A. Capozzoli, C. Curcio, G. D'Elia, and A. Liseno, "Fast phase-only synthesis of conformal reflectarrays," *IET Microw. Antennas Propag.*, vol. 4, no. 12, pp. 1989–2000, Dec. 2010.

[13] D. Pozar and D. Schaubert, "Analysis of an infinite array of rectangular microstrip patches with idealized probe feeds," *IEEE Trans. Antennas Propag.*, vol. AP-32, no. 10, pp. 1101–1107, Oct. 1984.

[14] R. Mittra, C. H. Chan, and T. Cwik, "Techniques for analyzing frequency selective surfaces—A review," *Proc. IEEE*, vol. 76, no. 12, pp. 1593–1615, Dec. 1988.

[15] D. M. Pozar, S. D. Targonski, and H. D. Syrigos, "Design of millimeter wave microstrip reflectarrays," *IEEE Trans. Antennas Propag.*, vol. 45, no. 2, pp. 287–296, Feb. 1997.

[16] J. A. Encinar, "Design of two-layer printed reflectarrays using patches of variable size," *IEEE Trans. Antennas Propag.*, vol. 49, no. 10, pp. 1403–1410, Oct. 2001.

[17] O. M. Bucci, A. Capozzoli, G. D'Elia, P. Maietta, and S. Russo, "An advanced reflectarray design technique," in *Proc. 28th ESA Antenna Workshop*, Noordwijk, The Netherlands, 2005.
[18] A. Capozzoli, C. Curcio, A. Liseno, M. Migliorelli, and G. Toso, "Aperiodic conformal reflectarrays," in *Proc. IEEE AP-S Int. Symp.*, Spokane, WA, USA, 2011.
[19] A. Capozzoli, C. Curcio, A. Liseno, M. Migliorelli, and G. Toso, "Power pattern synthesis of advanced flat aperiodic reflectarrays," in *Proc. 33th ESA Antenna Workshop*, Noordwijk, The Netherlands, 2011.
[20] O. M. Bucci, G. D'Elia, G. Mazzarella, and G. Panariello, "Antenna pattern synthesis: A new general approach," *Proc. IEEE*, vol. 82, no. 3, pp. 358–371, Mar. 1994.
[21] M. Zhou, S. B. Sørensen, E. Jørgensen, P. Meincke, O. S. Kim, and O. Breinbjerg, "An accurate technique for calculation of radiation from printed reflectarrays," *IEEE Antennas Wireless Propag. Lett.*, vol. 10, pp. 1081–1084, 2011.
[22] M. Zhou, S. B. Sørensen, O. S. Kim, S. Pivnenko, and G. Toso, "Investigations on accurate analysis of microstrip reflectarrays," in *Proc. 33rd ESA Antenna Workshop*, Noordwijk, The Netherlands, 2011.
[23] E. Jørgensen, J. Volakis, P. Meincke, and O. Breinbjerg, "Higher order hierarchical Legendre basis functions for electromagnetic modeling," *IEEE Trans. Antennas Propag.*, vol. 52, no. 11, pp. 2985–2995, Nov. 2004.
[24] M. Zhou, E. Jørgensen, O. S. Kim, S. B. Sørensen, P. Meincke, and O. Breinbjerg, "Accurate and efficient analysis of printed reflectarrays with arbitrary elements using higher-order hierarchical Legendre basis functions," *IEEE Antennas Wireless Propag. Lett.*, vol. 11, pp. 814–817, 2012.
[25] M. Arrebola, Y. Alvarez, J. A. Encinar, and F. Las-Heras, "Accurate analysis of printed reflectarrays considering the near field of the primary feed," *IET Microw. Antennas Propag.*, vol. 3, no. 2, pp. 187–194, 2009.
[26] DTU-ESA Spherical Near-Field Antenna Test Facility, [Online]. Available: http://www.dtu.dk/centre/ems/English/research/facilities.aspx
[27] *"POS, User's Manual. TICRA Engineering Consultants,"* 2011.
[28] J. A. Encinar and M. Arrebola, "Reduction of cross-polarization in contoured beam reflectarrays using a three-layer configuration," in *Proc. IEEE AP-S Int. Symp.*, Honolulu, HI, USA, 2007.
[29] C. Tienda, J. A. Encinar, M. Barba, and M. Arrebola, "Reduction of cross-polarization in offset reflectarrays using two layers of varying-sized patches," *Microw. Opt. Technol. Lett.*, vol. 54, no. 11, pp. 2449–2454, 2012.
[30] D. C. Chang and M. C. Huang, "Multiple-polarization microstrip reflectarray antenna with high efficiency and low cross-polarization," *IEEE Trans. Antennas Propag.*, vol. 43, no. 8, pp. 829–834, Aug. 1995.
[31] H. Hasani, M. Kamyab, and A. Mirkamali, "Low cross-polarization reflectarray antenna," *IEEE Trans. Antennas Propag.*, vol. 59, no. 5, pp. 1752–1756, May 2011.
[32] G. Kristensson, S. Poulsen, and S. Rikte, "Propagators and scattering of electromagnetic waves in planar bianisotropic slabs—An application to frequency selective structures," in *Progr. Electromagn. Res. (PIER)*, 2004, vol. 48, pp. 1–25.
[33] R. F. Harrington, *Time-Harmonic Electromagnetic Fields*. New York, NY, USA: McGraw-Hill, 1961.
[34] W. C. Chew and Q. Liu, "Resonance frequency of a rectangular microstrip patch," *IEEE Trans. Antennas Propag.*, vol. 36, no. 8, pp. 1045–1056, Aug. 1988.
[35] A. M. Lerer and A. G. Schuchinsky, "Full-wave analysis of three-dimensional planar structures," *IEEE Trans. Microw. Theory Tech.*, vol. 41, no. 11, pp. 2002–2015, Nov. 1993.
[36] S. R. Rengarajan, "Choice of basis functions for accurate characterization of infinite array of microstrip reflectarray elements," *IEEE Antennas Wireless Propag. Lett.*, vol. 4, pp. 47–50, 2005.
[37] S. M. Rao, D. R. Wilton, and A. W. Glisson, "Electromagnetic scattering by surfaces of arbitrary shape," *IEEE Trans. Antennas Propag.*, vol. AP-30, no. 3, pp. 409–418, May 1982.
[38] A. W. Glisson and D. R. Wilton, "Simple and efficient numerical methods for problems of electromagnetic radiation and scattering from surfaces," *IEEE Trans. Antennas Propag.*, vol. AP-28, no. 5, pp. 593–603, Sep. 1980.
[39] M. R. Chaharmir, J. Shaker, N. Gagnon, and D. Lee, "Design of broadband, single layer dual-band large reflectarray using multi open loop elements," *IEEE Trans. Antennas Propag.*, vol. 58, no. 9, pp. 2875–2883, Sep. 2010.
[40] M. R. Chaharmir, J. Shaker, and H. Legay, "Dual-band Ka/X reflectarray with broadband loop elements," *IET Microw. Antennas Propag.*, vol. 4, no. 2, pp. 225–231, 2010.
[41] M. Bozzi, S. Germani, and L. Perregrini, "Performance comparison of different element shapes used in printed reflectarrays," *IEEE Antennas Wireless Propag. Lett.*, vol. 2, no. 1, pp. 219–222, 2003.
[42] L. Marnat, R. Loison, R. Gillard, D. Bresciani, and H. Legay, "Accurate synthesis of a dual linearly polarized reflectarray," in *Proc. EuCAP*, Berlin, Germany, 2009.
[43] *Handbook of Mathematical Functions*, M. Abramowitz and I. A. Stegun, Eds., 9th ed. New York, NY, USA: Dover, 1970.
[44] *Spherical Near-Field Antenna Measurements*, J. E. Hansen, Ed. London, U.K.: Peter Peregrinus., 1988.
[45] S. D. Targonski and D. M. Pozar, "Analysis and design of a microstrip reflectarray using patches of variable size," in *Proc. IEEE AP-S Int. Symp.*, Seattle, WA, USA, 1994.
[46] "GRASP, Technical Description," K. Pontoppidan, Ed., TICRA Engineering Consultants, 2008.

**Min Zhou** (S'12) was born in Beijing, China, in 1984. He received the M.Sc. and Ph.D. degrees in electrical engineering from the Technical University of Denmark (DTU), Lyngby, in 2009 and 2013, respectively.

He is currently with TICRA, Copenhagen, Denmark. In fall 2007, he spent five months at the University of Illinois, Urbana-Champaign, IL, USA. His research interest include computational electromagnetics, antenna theory, and analysis and design techniques for printed reflectarrays.

**Stig B. Sørensen** was born in Denmark in 1958. He received the M.Sc. degree and the Industrial Research Education degree from the Technical University of Denmark (DTU), Lyngby, in 1982 and 1985, respectively.

Since 1983, he has been with TICRA, Copenhagen, Denmark, where he has been involved in the development of most of the TICRA software packages and the associated numerical electromagnetic methods. His research interests include computational electromagnetics, quasi-optical systems, and analysis and synthesis of shaped reflector antennas and printed reflectarrays.

**Oleksiy S. Kim** received the M.Sc. and Ph.D. degrees from the National Technical University of Ukraine, Kiev, in 1996 and 2000, respectively, both in electrical engineering.

In 2000, he joined the Antenna and Electromagnetics Group, Technical University of Denmark (DTU), Lyngby. He is currently an Associate Professor with the Department of Electrical Engineering, Electromagnetic Systems, DTU. His research interests include computational electromagnetics, metamaterials, electrically small antennas, photonic bandgap, and plasmonic structures.

**Erik Jørgensen** (S'98–M'03) was born in Denmark, in 1974. He received the M.Sc. and Ph.D. degrees in electrical engineering from the Technical University of Denmark (DTU), Lyngby, in 2000 and 2003, respectively.

In fall 1998, he spent five months at the University of Siena, Italy. In fall 2001, he was a Visiting Scholar at the Radiation Laboratory, University of Michigan, Ann Arbor. In 2003, he joined the TICRA, Copenhagen, Denmark, where he is now leading the development of commercial software for reflector antenna analysis and antenna diagnostics. His research interests include computational electromagnetics and high-frequency techniques.

**Peter Meincke** (S'93–M'96) was born in Roskilde, Denmark, on November 25, 1969. He received the M.Sc. and Ph.D. degrees in electrical engineering from the Technical University of Denmark (DTU), Lyngby, in 1993 and 1996, respectively.

In spring and summer of 1995, he was a Visiting Research Scientist at the Electromagnetics Directorate of Rome Laboratory, Hanscom Air Force Base, MA. In 1997, he was with a Danish cellular phone company, working on theoretical aspects of radio-wave propagation. In spring and summer of 1998, he was visiting the Center for Electromagnetics Research, Northeastern University, Boston, MA, while holding a Postdoctoral position from DTU. In 1999, he became a staff member of the Department of Electromagnetic Systems, DTU. He was an Associate Professor with Ørsted-DTU, Electromagnetic Systems, DTU, where his teaching and research interests included electromagnetic theory, inverse problems, high-frequency and time-domain scattering, antenna theory, and microwave imaging. Since 2008, he has been with TICRA, Copenhagen, Denmark, where he is currently developing software for reflector antenna analysis and antenna diagnostics.

Dr. Meincke won the first prize award in the 1996 IEEE Antennas and Propagation Society Student Paper Contest in Baltimore, MD, for his paper on uniform physical theory of diffraction equivalent edge currents and received the R.W.P. King Paper Award in 2000 for his paper "Time-domain version of the physical theory of diffraction" published in IEEE TRANSACTIONS ON ANTENNAS AND PROPAGATION, February, 1999.

**Olav Breinbjerg** (M'87) was born in Silkeborg, Denmark, in 1961. He received the M.Sc. and Ph.D. degrees in electrical engineering from the Technical University of Denmark (DTU), Lyngby, in 1987 and 1992, respectively.

Since 1991, he has been on the Faculty of the Department of Electrical Engineering as Assistant Professor from 1991 to 1995, Associate Professor from 1995 to 2005, and Full Professor since 2006. He is now Head of the Electromagnetic Systems Group and the DTU-ESA Spherical Near-Field Antenna Test Facility. He was a Visiting Scientist at Rome Laboratory in 1988, a Fulbright Research Scholar at the University of Texas at Austin in 1995, and a Visiting Professor at the University of Siena in 2011. He has been, or is, the main supervisor of 12 Ph.D. projects. His research is generally in applied electromagnetics—and particularly in antennas, antenna measurements, computational techniques, and scattering—for applications in wireless communication and sensing technologies. He is the author or coauthor of more than 50 journal papers, 150 conference papers, and 75 technical reports.

Dr. Breinbjerg received a U.S. Fulbright Research Award in 1995. He also received the 2001 AEG Elektron Foundation's Award in recognition of his research in applied electromagnetics and the 2003 DTU Student Union's Teacher of the Year Award for his course on electromagnetics.